COO-1789-1

CYCLOTRON WAVE PLASMA STUDIES

AEC Contract AT(11-1)-1789 Final Report

December 1, 1970

J. E. Scharer and J. B. Beyer, Principal Investigators
Ching-shie Horng, Graduate Student

The University of Wisconsin
Madison, Wisconsin

OBJECTIVES:

This is a final report on work done under AEC contract AT-(11-1)-1789. The objective of this project is to improve the diagnostic measurement of plasma density and collisional frequency in the presence of a magnetic field. To achieve the above objective the gridded electrodes and 10GHz microwave transmitting and receiving antennas were re-designed and the correlation of the theoretical model with the measurements has been made. As an alternative, a 35GHz Fabry-Perot cavity resonator system was constructed. The plasma was a cold collisional plasma in the presence of a magnetic field with an assumed relaxation collisional model. An electromagnetic wave was propagated along a uniform static magnetic field with a propagation phase constant β_p and an attenuation constant α_p.

DISCLAIMER

I. THEORY OF THE DIAGNOSTICS

A. Microwave interferometer measuring system.

In this system shown in Fig. 1 a plasma slab model was considered. The plasma slab is created by the electrical glow discharge over a pair of microwave-transparent gridded electrodes back-insulated by dielectric sheet and separated each other by a distance d as shown in Fig. 2. The discharge current source is from a charged capacitor of 14 μfd and the discharge period can be controlled from several micro-seconds to milliseconds by switching off the source at a proper time. To determine the density n and the collisional frequency ν_{en} in the after-glow, a right-hand circularly polarized wave of frequency 10 GHz was normally incident on the plasma slab, multi-reflected back and forth in the slab, and finally transmitted through the slab reaching the receiving antenna. The total complex wave reflection coefficient r and transmission coefficient t were shown to be the following:

$$r = \frac{E_r}{E_i} = \frac{(1-K^{\frac{1}{2}})(1+K^{\frac{-1}{2}}) + (1+K^{\frac{1}{2}})(1-K^{\frac{-1}{2}})e^{-j2(\beta_p - j\alpha_p)d}}{(1+K^{\frac{1}{2}})(1+K^{\frac{-1}{2}}) + (1-K^{\frac{1}{2}})(1-K^{\frac{-1}{2}})e^{-j2(\beta_p - j\alpha_p)d}} \qquad (1)$$

$$t = \frac{E_t}{E_i} = \frac{4\, e^{j\beta_o d}}{(1-K^{\frac{1}{2}})(1-K^{\frac{-1}{2}})e^{-j(\beta_p - j\alpha_p)d} + (1+K^{\frac{1}{2}})(1+K^{\frac{-1}{2}})e^{j(\beta_p - j\alpha_p)d}} \qquad (2)$$

where $K^{1/2}$ is the ratio of the wave impedance in the plasma to that in the vacuum, β_o is the propagation phase factor of the wave in

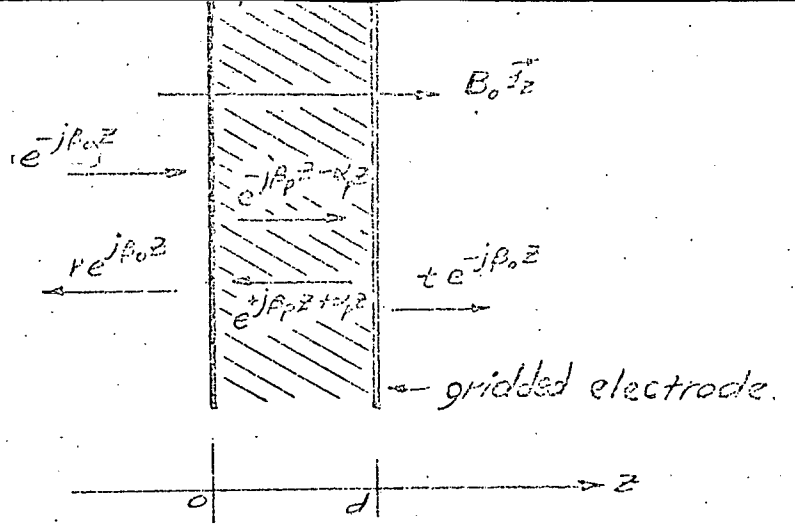

Fig. 1 plasma slab

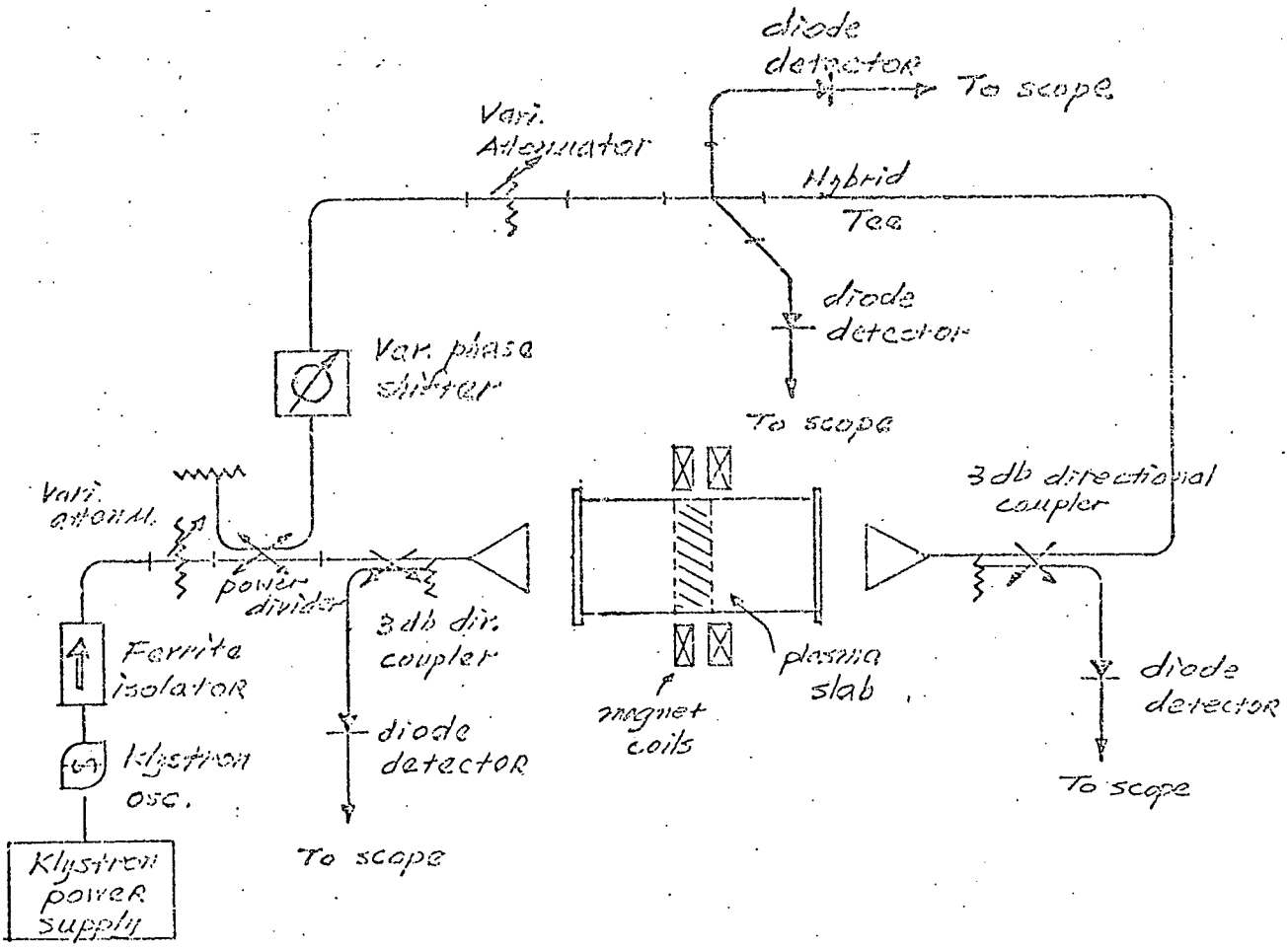

Fig. 2 schematic diagram of microwave interferometer

vacuum and β_p in the plasma. α_p is the attenuation constant of the wave in the plasma and d is the thickness of the plasma slab. The total reflection and transmission power coefficients can be written in the form:

$$R = |r|^2 = \frac{\sin^2\beta_p d + \sinh^2\alpha_p d}{\sin^2(\beta_p d+\delta)+\sinh^2(\alpha_p d+s)} \tag{3}$$

$$T = |t|^2 = \frac{\sin^2\delta + \sinh^2 s}{\sin^2(\beta_p d+\delta)+\sinh^2(\beta_p d+s)} \tag{4}$$

where

$$\delta=\tan^{-1}\frac{-2\alpha_p\beta_o}{\beta_o^2-(\alpha_p^2+\beta_p^2)} \quad \text{and} \quad s = -\frac{1}{2}\ell n\frac{\alpha_p^2+(\beta_o-\beta_p)^2}{\alpha_p^2+(\beta_o+\beta_p)^2}$$

The phase and the amplitude components in equation (1) and (2) can be measured by the interferometer and the R and the T can be simply detected by the diodes. Hence β_p and α_p can be solved in terms of measured quantities; further, the density n and the collisional frequency can be solved in terms of β_p and α_p.

B. Fabry-Perot resonator measuring system

Shown in Fig. 3 is a microwave measuring system and Fabry-Perot resonator, made of a pair of spherical mirrors with radius 20" and diameter 6 inches. The resonator is filled with a uniform cold magneto-plasma of density n and collisional frequency ν_{en} which is created by the glow-discharge over the surfaces of the mirror. The resonator is excited with a plane polarized wave from the center of one of the mirrors, and the resonator resonant frequency and the Q in this plasma medium are given below:

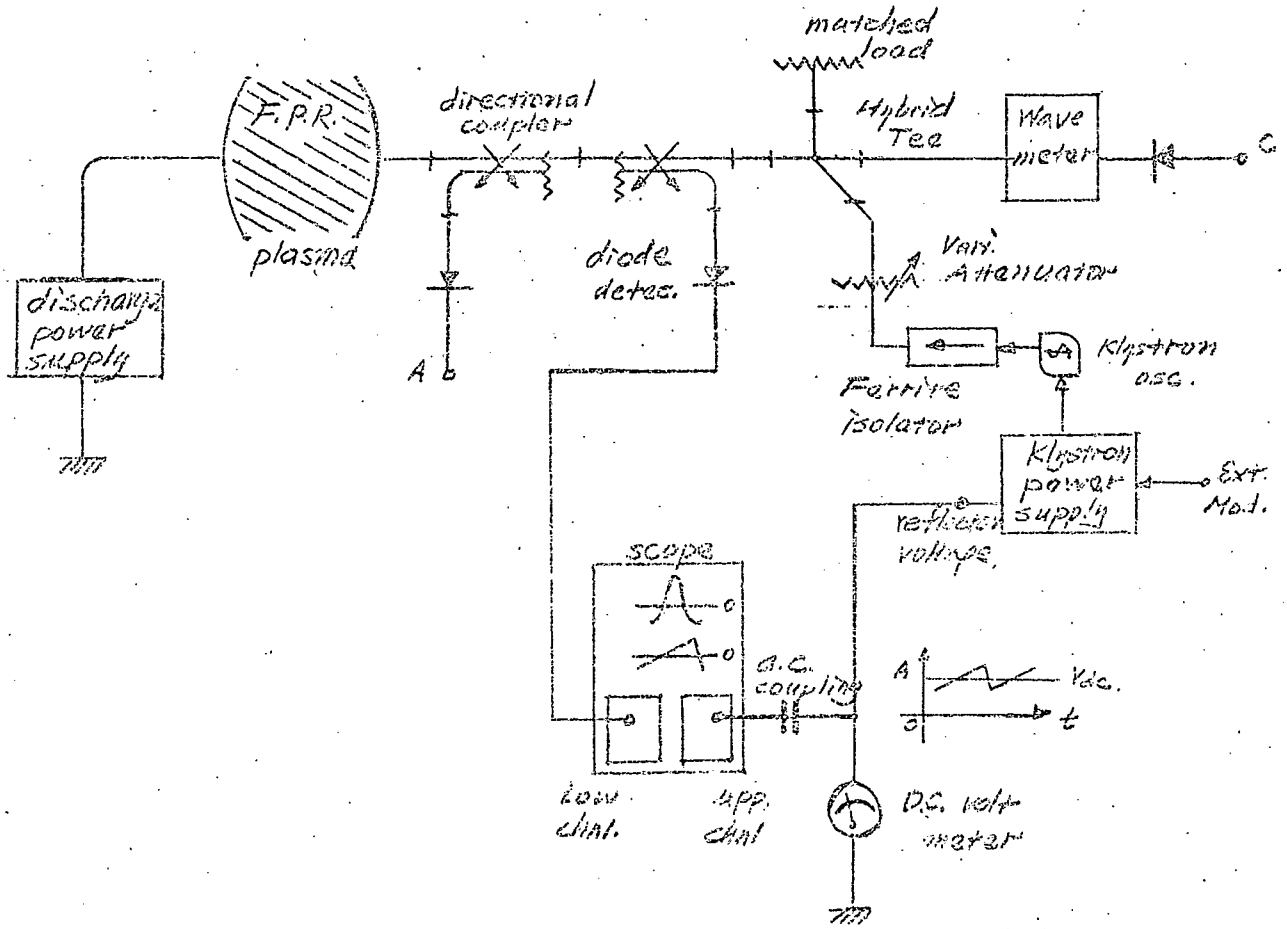

Fig. 3 Basic microwave detection system for Fabry-Perot

$$\mu^2 = \frac{\text{cons}^2}{\omega_o^2} = \left[\frac{1}{2}\left(1 - \frac{\omega_p^2(\omega_o \mp \omega_b)}{\omega_o[(\omega_o \mp \omega_b)^2 + \nu_{en}^2]}\right)\right.$$

$$\left. + \frac{1}{2}\left(\left[1 - \frac{\omega_p^2(\omega_o \mp \omega_b)}{\omega_o[(\omega_o \mp \omega_b)^2 + \nu_{en}^2]}\right]^2 + \left[\frac{\omega_p^2 \nu_{en}}{\omega_o[(\omega_o \mp \omega_b)^2 + \nu_{en}^2]}\right]^2\right)^{\frac{1}{2}}\right]^{\frac{1}{2}}$$

$$Q = \frac{2\pi d}{\lambda_p(1-e^{-2\alpha d})} \tag{5}$$

If the collision frequency is sufficiently small and the operating frequency is far from the electron cyclotron frequency, a simplified expression can be obtained in the following form:

$$\mu^2 = \frac{\text{cons}^2}{\omega_o^2} = 1 - \frac{\omega_p^2}{\omega_o(\omega_o \mp \omega_b)}$$

or $$\omega_o^3 \mp \omega_b \omega_o^2 - (\omega_p^2 + \text{cons}^2)\,\omega_o \pm \omega_b\,\text{cons}^2 = 0$$

In the above equation, the upper sign stands for lhcp wave; the lower the rhcp wave. By measuring both resonant frequencies of the rhcp and lhcp waves, the parameters of the resonator geometry can be eliminated and the plasma density can be found from the following equation:

$$\omega_p^2 = (\omega_r - \omega_b)\,(\omega_\ell + \omega_b)\Delta\omega/\omega_b \quad \text{where } \Delta\omega = \omega_r - \omega_\ell$$

II. EXPERIMENTAL RESULTS

A theory which relates plasma slab and measurement data has been worked out on the basis of Appleton-Hartree cold plasma model in the range of $Y = \omega_{ce}/\omega$ from 0 to 1.2 corresponding to the maximum available static B-field. The discharge system operates at from 1 to 2 kv source voltage from the discharge of a 14 μfd capacitor. The first problem to be solved is to improve the arcing and then to obtain a high density plasma. The arcing conditions for this system were visually observed and the v-i curve of the discharge was photographed at various gas pressure so that the arcing voltage and discharge current could be noted and then compared with the later improvements. The nonuniform discharge over the electrode grid planes lead to the possibility of the use of a tougher insulation material such as mica. Through many tests it was found that to avoid arcing the geometry of the gridded electrodes should be such that the diameter of the back-insulation plates is larger than the diameter of the grid and equal to the diameter of the glass pipe. Furthermore the plates should be placed about 1/8" to 1/4" from the grid. At this stage the source discharge voltage from the capacitor raised from 4 to 6 Kv from the previous 2Kv for a fixed spacing of the electrodes for various pressure range without arcing difficulties. With the new construction of the gridded electrodes, a formal experiment was done, but the results were still not satisfactory on one point. This was that the transmission coefficient T when the plasma was discharged was greater than unity for a given $Y = \omega_{ce}/\omega$. This was overcome by wrapping the pipe in the region between the two grids with electrically floating aluminum foil strips about 1 inch wide and a half inch separation.

DATA

1. v-i curve of the discharge

Conditions under which the curve is obtained

1. the circuit arrangement

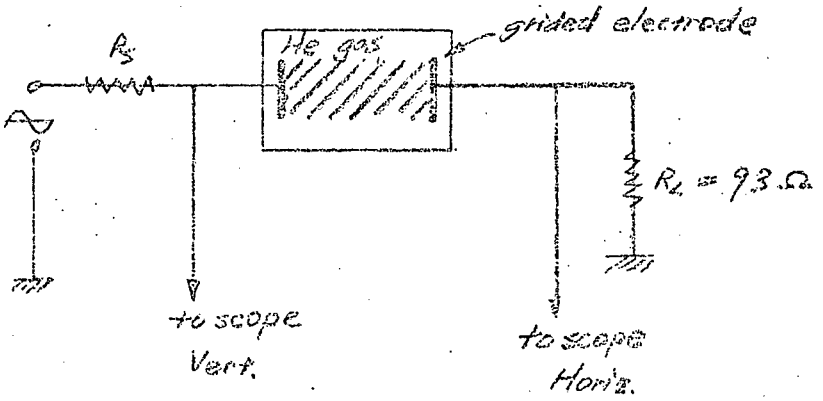

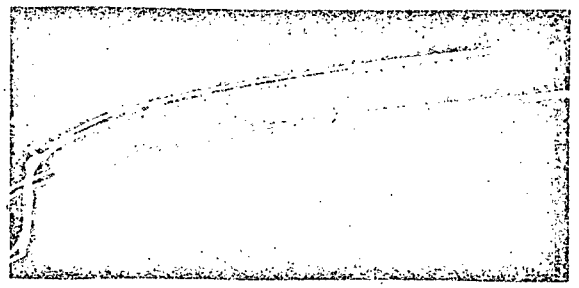

scope settings:
horizontal channel - 2 volts/cm
vertical channel - 1 kvolts/cm

gas pressure:
32.5-33 mm of Hg. (valve opening at 5 micrometer.)

upper trace:
immediately before arcing

low trace:
arc over teflon wedge at the wall of the glass pipe.

Fig. 4

Later, the original antenna horn was extended and a set of the plane-hyperbola lenses were fabricated to confine the beam of the wave, eliminating the stray path between the receiving and the transmitting antenna. The antenna patterns of the extended horn with and without lenses were obtained.

In order to obtain an even narrower beam angle and field distribution similar to that in the Fabry-Perot system, a second set of the lenses was studied. A new Fabry-Perot resonator with a 20" spherical mirror radius and a 6" diameter was fabricated. And a microwave measurement system was designed to obtain the resonant frequency and Q of the cavity. In order to obtain more accurate measurements the resonance curve is directly displayed on the scope screen by sweeping the klystron reflector voltage. And at the same time, the klystron reflector voltage is displayed on the lower channel to mark the frequency axis.

III. Comparison of the Microwave Interferometer System and Fabry-Perot Resonator Methods of Plasma Diagnostics.

To simplify the conditions involved, assume first that the antenna system of the interferometer radiates the field with the distribution the same as that in the Fabry-Perot resonator, whose field distribution can be obtained by proper lens correction. Now the comparison point is on the data measurements. For the interferometer system, the density and collisional frequency can be determined either from the measurement of the power transmission and reflection coefficient or from the measurement of the

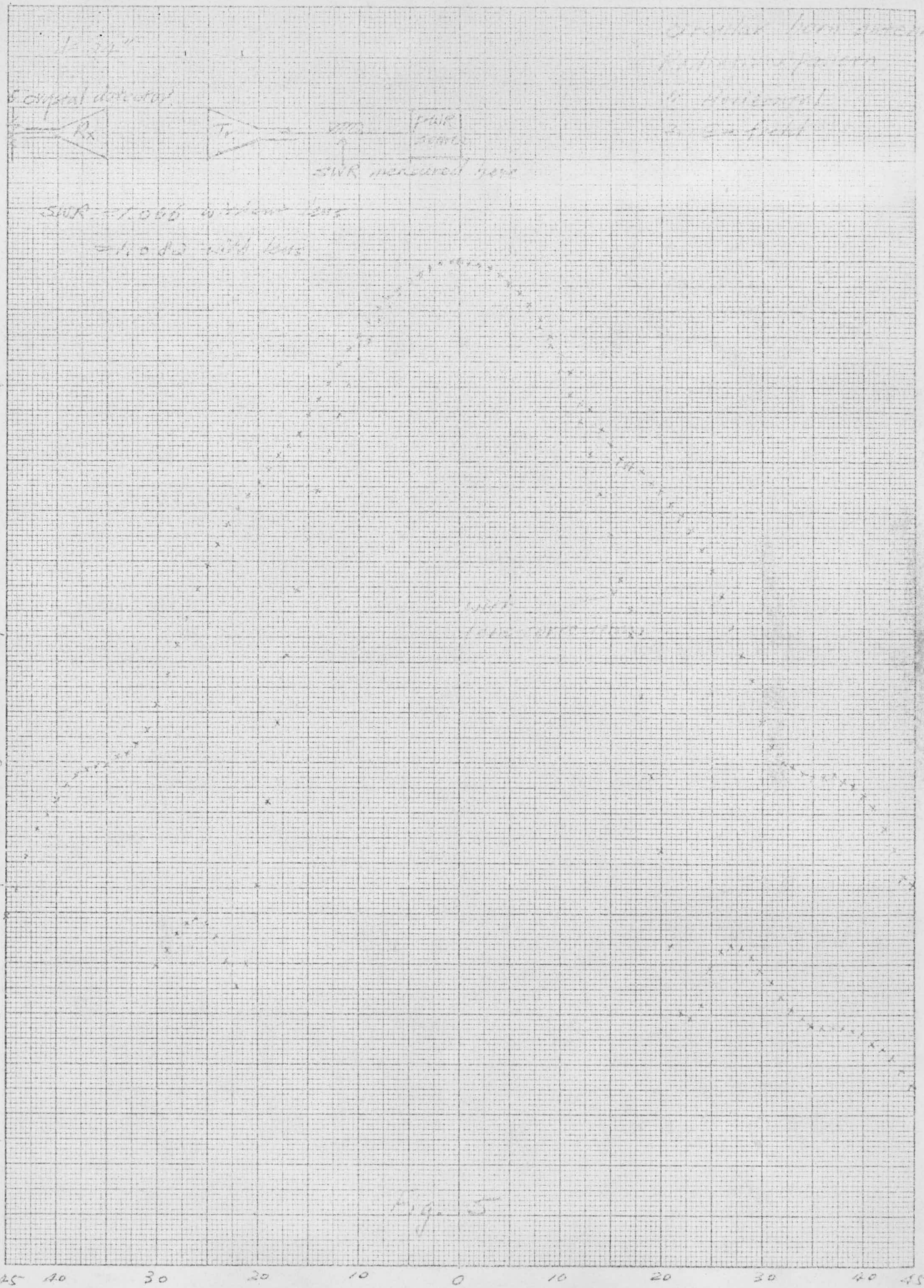

phase and the amplitude components of the transmission coefficient, while for the Fabry-Perot resonator, the density and collisional frequency can be determined by the resonant frequency and cavity Q. If the plasma is transient, the first corresponds to the measurement of phase modulated signal and the second to the measurement of frequency modulated signal. As far as volume is concerned, the Fabry-Perot mirrors and lens corrected horns may occupy the same space for a certain confinement of the wave beam at a fixed frequency. For the slab model of the interferometer system, the slab width is a first order quantity and the slab walls must be parallel. For the Fabry-Perot system the plasma dimensions and the shape is not important as long as the plasma is a small perturbation to the cavity. For practical applications, the interferometer system needs at least one microwave transparent diagnostic port. In contrast, the Fabry-Perot mirrors can be a part of the plasma containing walls if the plasma is confined in a metal wall with sufficient conductivity.

In conclusion, the main advantage of the Fabry-Perot system is that the exact plasma geometry and the homogenity involved is not important for a small cavity perturbation.

List of Notations.

α_p = attenuation constant

β_o, β_p = propagation phase constant in the free space and in the plasma respectively.

r = reflection coefficient

t = transmission coefficient

$K^{\frac{1}{2}}$ = the ratio of the wave impedance in the plasma to that in the vacuum.

d = the plasma slab thickness in slab model or the separation of Fabry-Perot (shorted as F.P.) mirrors.

$\mu = \frac{\beta_p}{\beta_o}$ = refraction index

ω_p = plasma frequency

ω_b or ω_{ce} = electron cyclotron frequency at B-field, $\bar{B}_z$.

ω_r = resonant frequency of F.P. for rhcp wave

ω_r = resonant frequency of F.P. for lhcp wave

ω_o = resonant frequency of F.P.
$\omega_o = \omega_l$ when upper sign was adopted in the equations
$\omega_o = \omega_r$ when lower sign was adopted in the equations

cons = a constant related to the F.P. geometry and dimension equals to $\frac{\pi C(m + 1/2)}{d}$ where C is the speed of light, and m is the resonance mode number.

λ_p = $\frac{2\pi}{\beta_p}$